BMC Medical Imaging

RESEARCH

Open Access

Prediction of PD-L1 and Ki-67 status in primary central nervous system diffuse large B-cell lymphoma by diffusion and perfusion MRI: a preliminary study

Xiaofang Zhou[1,2†], Feng Wang[1,2†], Lan Yu[1,2], Feiman Yang[1,2], Jie Kang[1,2], Dairong Cao[1,2,3,4*†] and Zhen Xing[1,2*†]

Abstract

Objective To assess whether diffusion and perfusion MRI derived parameters could non-invasively predict PD-L1 and Ki-67 status in primary central nervous system diffuse large B-cell lymphoma (PCNS-DLBCL).

Methods We retrospectively analyzed DWI, DSC-PWI, and morphological MRI (mMRI) in 88 patients with PCNS-DLBCL. The mMRI features were compared using chi-square tests or Fisher exact test. Minimum ADC (ADC_{min}), mean ADC(ADC_{mean}), relative minimum ADC ($rADC_{min}$), relative mean ADC ($rADC_{mean}$), and relative maximum CBV ($rCBV_{max}$) values were compared in PCNS-DLBCL with different molecular status by using the Mann-Whitney U test. The diagnostic performances were evaluated by receiver operating characteristic curves.

Results PCNS-DLBCL with high PD-L1 expression demonstrated a significantly higher ADC_{min} value than those with low PD-L1. The ADC_{mean} and $rADC_{mean}$ values were significantly lower in PCNS-DLBCL with high Ki-67 status compared with those in low Ki-67 status. Other ADC, CBV parameters, and mMRI features did not show any association with these molecular statuses The diagnostic efficacy of ADC values in assessing PD-L1 and Ki-67 status was relatively low, with area under the curves (AUCs) values less than 0.7.

Conclusions DWI-derived ADC values can provide some relevant information about PD-L1 and Ki-67 status in PCNS-DLBCL, but may not be sufficient to predict their expression due to the rather low diagnostic performance.

Keywords Lymphoma, Programmed cell death ligand-1, Ki-67, Magnetic resonance imaging

†Xiaofang Zhou and Feng Wang contributed equally to this work and are co-first authors.

†Dairong Cao and Zhen Xing contributed equally to this work.

*Correspondence:
Dairong Cao
dairongcao@163.com
Zhen Xing
anight306@126.com

[1]Department of Radiology, The First Affiliated Hospital of Fujian Medical University, 20 Cha-Zhong Road, Fuzhou 350005, Fujian, P.R. China
[2]Department of Radiology, Binhai Campus of the First Affiliated Hospital, National Regional Medical Center, Fujian Medical University, Fuzhou 350212, Fujian, China
[3]Department of Radiology, Fujian Key Laboratory of Precision Medicine for Cancer, the First Affiliated Hospital, Fujian Medical University, Fuzhou 350005, China
[4]Key Laboratory of Radiation Biology of Fujian Higher Education Institutions, the First Affiliated Hospital, Fujian Medical University, Fuzhou 350005, China

Introduction

Primary central nervous system lymphoma (PCNSL), an extra-nodal entity of non-Hodgkin lymphoma restricted to the CNS [1], accounts for approximately 5% of newly diagnosed intracranial tumors with rising incidence in the last decades [2, 3], and more than 90% of them are categorized as diffuse large B-cell lymphoma (DLBCL) [4]. Primary central nervous system DLBCL (PCNS-DLBCL) has more aggressive biology behaviors and heterogenous genetic features with a poorer clinical outcome compared to systemic DLBCL [5]. Due to its marked heterogeneity, around 30–40% of PCNS-DLBCL cases exhibit resistance towards the conventional treatment approach of rituximab and anthracycline-based chemotherapies, leading to subsequent relapse or refractory diseases [6]. Hence, the identification of novel therapeutic targets and supplementary biomarkers for relapse or refractory DLBCL assumes utmost significance.

Recently, the immune checkpoint inhibitors targeting programmed cell death-1 (PD-1)/programmed cell death ligand-1 (PD-L1) pathway have emerged as a highly promising therapeutic approach for haematolymphoid malignancies [7–12], including classical Hodgkin lymphoma, follicular lymphoma, as well as potential utility in DLBCL, renewing the hope for the patients with relapsed or refractory lymphoma. Nevertheless, a considerable percentage of patients receiving checkpoint inhibitors exhibit minimal or negligible efficacy while these treatments might have associated toxicities and are costly. Currently, PD-L1 expression in tumor cells, a predictor of treatment response and prognosis, has been proven to be the most prevalent biomarker for optimizing patient selection [7, 13, 14]. Ki-67 labeling index (LI), a cell nuclear antigen associated with the proliferative activity of the tumor, has been widely represented as a prognostic predictor for DLBCL [15]. Previously, studies reported that PD-L1 expression was significantly correlated with Ki-67 LI in solid tumors [16, 17]. Therefore, early identification of PD-L1 and Ki-67 status can aid in treatment decision-making and providing prognostic information.

Currently, the gold standard for assessing PD-L1 and Ki-67 is predominantly through immunohistochemical staining (IHC) of biopsy specimens or surgical resection, which is limited in patients with compromised health due to its invasiveness, time-consuming, tumor heterogeneity and unrepeatability. Additionally, obtaining tissue samples from inaccessible sites can pose challenges in certain cases. Consequently, there is a need to explore a novel, precise, and noninvasive approach for evaluating these factors in the clinic. Physiology-based MR imaging, such as diffusion weighted imaging (DWI) and dynamic susceptibility contrast perfusion-weighted imaging (DSC-PWI), are used clinically to characterize microstructural features of biological tissues. Previous studies have indicated that the DWI-derived apparent diffusion coefficient (ADC) values are significantly correlated with Ki-67 LI in various tumors, such as soft tissue sarcoma, sinonasal malignancies, endometrial carcinoma, and PCNSL. Moreover, ADC values have been found to have a statistically significant association with PD-L1 expression in head and neck squamous cell carcinomas (HNSCC)) [18–24]. In addition, DSC-derived cerebral blood volume (CBV) values are statistically associated with Ki-67 LI in meningiomas and gliomas [25–27]. However, to the best of our knowledge, the correlation of DWI and DSC-PWI with PD-L1 and Ki-67 expression in PCNS-DLBCL has not been extensively studied.

Therefore, this study aims to investigate whether preoperative diffusion and perfusion parameters can effectively predict PD-L1 and Ki-67 expression in PCNS-DLBCL.

Materials and methods

Patients

This study received approval from the Medical Ethics Committee of the First Affiliated Hospital of Fujian Medical University, and the requirement for patient informed consent was waived. 148 patients with histologically confirmed PCNS-DLBCL from May 2019 to June 2023 were consecutively enrolled according to the following inclusion criteria: (1) histopathologic diagnosis of PCNS-DLBCL through stereotactic biopsy or surgical resection according to the 2021 WHO classification; (2) Preoperative standard MRI were examined. The exclusion criteria included: (1) PD-L1 and Ki-67 status were unavailable from pathology ($n=40$); (2) the patient had experienced a recurrence or received therapeutic intervention before MRI examination ($n=6$); (3) MRI performed in <3.0T MRI scanner ($n=6$); and (4) MRI data was missing or the image quality was poor ($n=8$). Ultimately, 88 patients (39 males and 49 females; mean age, 61.92±9.33 years; age range, 32–80 years) were enrolled. All patients underwent mMRI and DWI; 76 patients underwent DSC-PWI.

MRI protocols

MRI examinations were performed with 3.0 T MRI system (Verio, Prisma, or Skyra; Siemens, Erlangen, Germany). Morphological MRI (mMRI) protocols included axial T1-weighted imaging (TR/TE=250/2.48 ms), axial T2-weighted imaging (TR/TE=4000/125 ms), axial fluid-attenuated inversion recovery imaging (TR/TE=9000/94 ms), and contrast-enhanced T1-weighted imaging (TR/TE=250/2.48 ms). Uniform imaging parameters were maintained across all sequences, with a FOV of 220×220 mm, a slice thickness of 5 mm, a matrix size of 256×256, and an intersection gap of 1 mm, as proposed in our previous studies [26–28].

DWI was conducted with an axial echo-planar sequence in all 3 orthogonal diffusion directions

according to the following technique parameters: b values, 0 and 1000s/mm^2; TR/TE, 8200/102; matrix, 128×128; FOV, 220×220 mm; number of excitations, 2.0; slice thickness, 5 mm; slice spacing, 1 mm; ADC maps were calculated automatically using MRI post-processing workstation.

DSC-PWI was examined with a gradient-recalled T2*-weighted echoplanar imaging sequence using a standard dose of 0.1 mmol/kg of gadobenate dimeglumine at a rate of 5 mL/s. DSC-PWI was conducted using the main perfusion dose after a full-dose contrast agent preload. The parameters were as follows: TR range/TE, 1000–1250/54; matrix, 128×128; FOV, 220×220 mm; number of excitations, 1.0; slice thickness, 5 mm; slice spacing, 1 mm; flip angle, 90°. The CBV map was extracted from time-intensity curves by dynamic monitoring of T2* signal intensity changes during contrast administration. A global clustering algorithm was utilized to examine the time series data from all voxels, facilitating the identification of an appropriate local arterial input function. Subsequently, the arterial input function was automatically generated for each distinct dataset. The algorithm provided by Syngo. Via was used to correct for T1 leakage effects. The CBV map was reconstructed automatically using the "single-compartment model" and the deconvolution algorithm for exogenous perfusion.

MRI analysis

The mMRI features were independently analyzed in consensus by two radiologists respectively (L.Y and X.Z with 2 and 6 years of experience in neuroimaging), who were blinded to IHC results. The following imaging features were recorded: tumor location (supratentorial or infratentorial; superficial or deep); tumor number (single or multiple); tumor size (largest diameter, in centimeters); degree of peritumoral edema; the presence of necrosis; the presence of cystic degeneration; the presence of hemorrhage; enhancement pattern (none/mild or marked; heterogeneous or homogeneous); tumor margin (well-defined or poorly-defined). Tumor size was determined by measuring the largest diameter of the tumor on axial contrast-enhanced T1-weighted imaging. Edema was classified into three categories based on its maximum distance from the tumor edge: not apparent (less than 1 cm), mild to moderate (between 1 cm and 2 cm), and severe (greater than 2 cm). The imaging features descriptors were established based on the VASARI (Visually Accessible Rembrandt Images) feature scoring system.

Another senior radiologist (Z.X, with 13 years of experience in neuroimaging) blinded to IHC results evaluated the ADC and CBV maps separately using an off-line syngo B19 workstation (syngo; Siemens, Erlangen, Germany). Five non-overlapping ROIs (20 to 25 mm$^{\wedge 2}$) were manually drawn on the ADC maps in regions exhibiting the visually lowest ADC values within the solid components of the tumors. Areas with hemorrhage, necrosis, calcification, cystic degeneration, blood vessels, and sulci were carefully excluded during the ROI placement. The lowest ADC value among the five ROIs was chosen as the minimum ADC (ADC_{min}) value, and the average ADC value of ROIs was considered mean ADC (ADC_{men}) value. Additionally, three similarly sized ROIs were placed on ADC maps within the contralateral normal-appearing white matter to calculate their average values. To reduce patient-specific variations, the minimum relative ADC ($rADC_{min}$) and mean relative ADC ($rADC_{mean}$) values were determined by normalizing the tumor ADC_{min} and ADC_{mean} values against the mean ADC values of contralateral normal-appearing white matter. Similarly, the maximum relative CBV ($rCBV_{max}$) values were derived using the same normalization approach applied to the ADC measurements. To evaluate the inter-observer agreement, the neuroradiologist (J.K, with 3 years of experience) consistently measured the diffusion and perfusion parameters across all patients. To evaluate intra-observer consistency, Z.X measured the diffusion and perfusion parameters repeatedly with a minimum interval of 1 month. The initial data set collected by Z.X was subsequently employed for further statistical analysis.

IHC analysis of the PD-L1 and Ki-67 expression

PD-L1 and Ki-67 status were retrospectively obtained from pathological reports. PD-L1 expression was evaluated on formalin-fixed paraffin-embedded biopsy or surgical specimen, and IHC test was performed with PD-L1 IHC 28−8 pharm Dx Kit. (Monoclonal mouse anti-human antibody, Clone 28−8, Abcam PLC, UK) The PD-L1 high expression was defined as the percentage of PD-L1-positive tumor cells relative to the total tumor cells exceeding 30%; otherwise, it was defined as PD-L1 low expression [13]. Ki-67 LI was also detected by hematoxylin-eosin staining as previously described. Briefly, a quantitative estimation was determined based on the percentage of positive cells in the area with the highest number of positive nuclei of stained cells. Ki-67 expression levels were classified as either low (Ki-67 LI≤70%) or high Ki-67 status (Ki-67 LI>70%) in our study [15].

Statistical analysis

The Kolmogorov-Smirnov tests were first used to assess the normality of all continuous parameters. All data were represented as medians (interquartile range), means (standards deviation), or numbers of cases and ratios, appropriately. The inter- and intra-reader reproducibility of diffusion and perfusion parameter measurements were assessed using the intraclass correlation coefficient

Table 1 Clinical, mMRI features, diffusion, and perfusion MRI parameters of different molecular status in the patients of PCNS-DLBCL

	PD-L1			Ki-67		
	Low (63)	High (25)	*P*	Low (15)	High (73)	*P*
Age(yr)	62.94 ± 9.75	59.36 ± 7.78	0.034	60.53 ± 7.61	62.21 ± 9.67	0.383
Gender (Male/Female)	26/37	13/12	0.361	8/7	31/42	0.440
Location						
Supratentorial/ infratentorial	54/9	22/3	1.000	13/2	63/10	1.000
Superficial/ deep	49/14	20/5	0.819	13/2	56/17	0.508
Lesion number (Single/ multiple)	20/43	9/16	0.702	3/12	26/47	0.367
Conventional MR imaging						
Size(cm)	3.02 ± 1.28	3.14 ± 1.69	0.926	2.84 ± 1.45	3.10 ± 1.39	0.515
Peritumoral edema			0.353			0.645
Not apparent (< 1 cm)	8	6		1	13	
Mild to moderate (> 1 cm and < 2 cm)	12	5		3	14	
Severe (> 2 cm)	43	14		11	46	
Presence of necrosis (No.) (%)	29(46.03%)	9(36.00%)	0.392	6(40.00%)	32(43.84%)	0.785
Presence of cystic degeneration (No.) (%)	0(0%)	1(4.00%)	0.284	0(0%)	1(1.37%)	1.000
Presence of hemorrhage (No.) (%)	24(38.10%)	6(24.00%)	0.208	4(26.67%)	26(35.62%)	0.505
Enhancement pattern						
None or mild/ marked	4/59	0/25	0.574	0/15	4/69	1.000
Heterogeneous/ homogeneous	18/45	5/20	0.439	3/12	20/53	0.750
Margin (well-defined/ poorly-defined)	41/22	12/13	0.155	8/7	45/28	0.574
ADC_{min}	0.586(0.531–0.669)	0.638(0.571–0.727)	0.038	0.650(0.586–0.723)	0.614(0.535–0.678)	0.050
ADC_{mean}	0.664(0.578–0.729)	0.688(0.631–0.772)	0.053	0.720(0.664–0.768)	0.653(0.581–0.734)	0.023
$rADC_{min}$	0.870(0.752–0.954)	0.925(0.808–1.012)	0.129	0.922(0.845–1.045)	0.870(0.750–0.957)	0.087
$rADC_{mean}$	0.931(0.842–1.019)	0.979(0.891–1.060)	0.186	1.011(0.921–1.185)	0.931(0.850–1.031)	0.037
$rCBV_{max}$	7.856(6.004–11.710)	7.939(5.779–12.280)	0.897	8.582(7.560–11.250)	7.456(5.721–11.808)	0.331

Note: ADC_{min}, ADC_{mean}, $rADC_{min}$, $rADC_{mean}$, and rCBVmax were presented as medians with interquartile ranges in parentheses; Low, PD-L1 ≤ 30%; High, PD-L1 > 30%; Low, Ki-67 LI ≤ 70%; High, Ki-67 LI > 70%

(ICC). The interobserver rater reliability coefficient of mMRI features was performed with Cohen's Kappa statistics. The clinical data, mMRI features, and parameters derived from diffusion and perfusion maps were compared between low or high PD-L1and Ki-67 status with the Mann-Whitney U tests or t-tests for continuous variables, and Fisher exact tests or chi-square tests for categoric variables, properly. Receiver-operating characteristic (ROC) curve analyses were made to determine the diagnostic efficacy of significant parameters for differentiating between low and high PD-L1 and Ki-67 status. The area under the curves (AUCs), sensitivity, and specificity of these significant parameters for differential diagnosis were calculated. The cutoff values for quantitative parameters that provided optimal sensitivity and specificity were defined. $P<0.05$ was indicated as statistically significant. Statistical analysis was performed utilizing IBM SPSS Statistics (version 25.0, IBM) and MedCalc Statistics (version 15.6, MedCalc).

Results

The clinical demographic characteristics, mMRI features, diffusion and perfusion MRI parameters of different PD-L1 and Ki-67 statuses are shown in Table 1. PCNS-DLBCL with a high PD-L1 expression showed increased incidence in younger patients ($P=0.034$), however, there was no significant difference in the low and high Ki-67status. No differences in gender and all mMRI imaging features were observed between different PD-L1 and Ki-67 expression status. Interobserver agreements for mMRI features were excellent (all kappa coefficient values > 0.80). Good intra-observer and inter-observer agreements for the measurement of DWI and DSC-PWI parameters were achieved, as presented in Table 2.

Table 2 Inter-observer and intra-observer reproducibility for measurements of diffusion and perfusion parameters

Parameters	ICC (95%CI)	
	Inter-observer	Intra-observer
ADC_{min}	0.863(0.791–0.910)	0.899(0.813–0.942)
ADC_{mean}	0.870(0.801–0.915)	0.868(0.806–0.912)
$rADC_{min}$	0.923(0.882–0.949)	0.914(0.868–0.943)
$rADC_{mean}$	0.910(0.862–0.942)	0.909(0.860–0.940)
$rCBV_{max}$	0.955(0.929–0.972)	0.964(0.943–0.977)

Note: Data in parentheses are the 95% confidence interval. ICC intraclass correlation coefficient, CI confidence interval

The results of the comparative analyses of DWI and DSC-PWI parameters between different PD-L1 and Ki-67 statuses in PCNS-DLBCL are shown in Table 1; Fig. 1. ADC_{min} values were significantly higher with

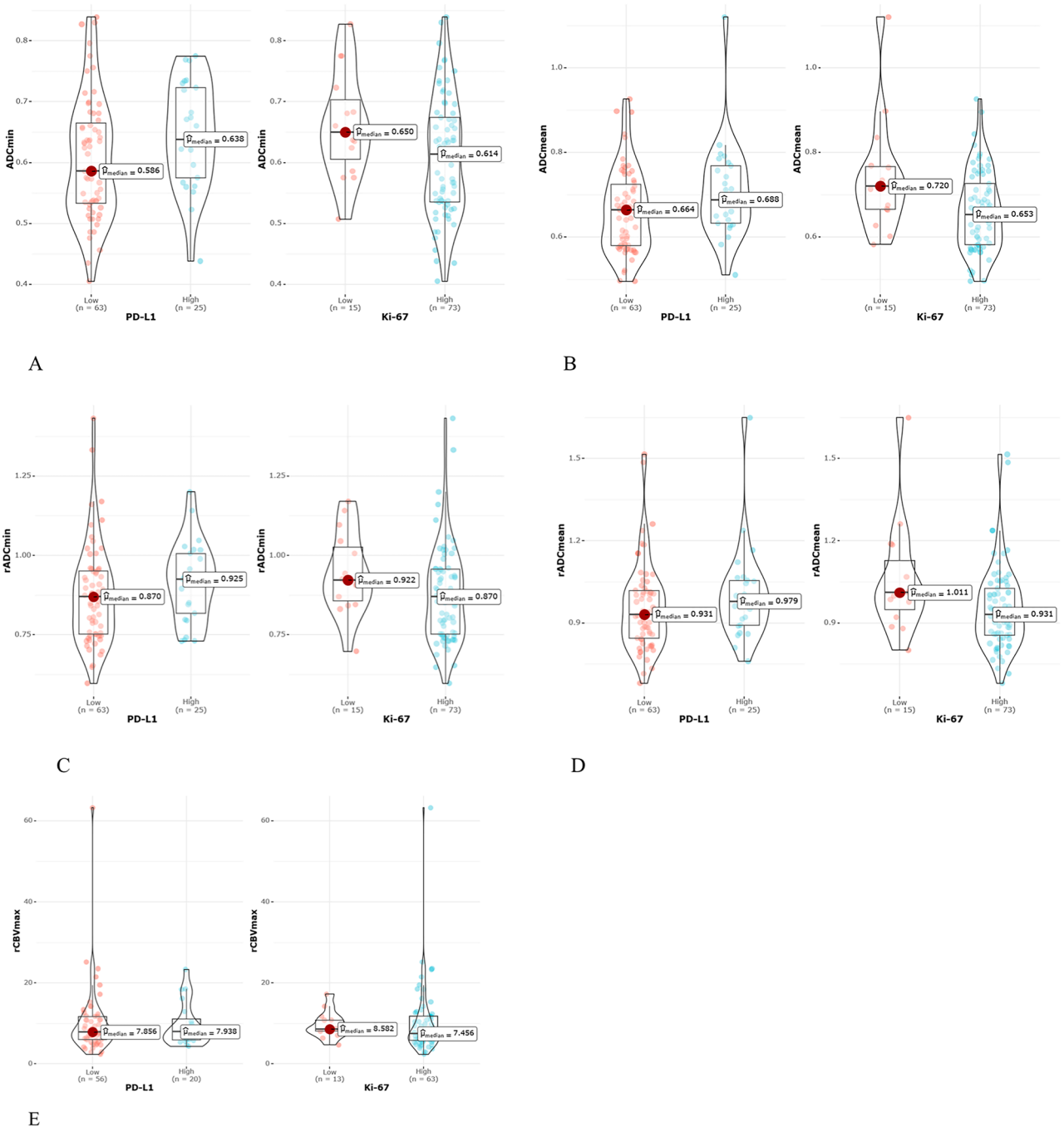

Fig. 1 Violin plots show distributions of ADC_{min} (**A**), ADC_{mean} (**B**), $rADC_{min}$ (**C**), $rADC_{mean}$ (**D**), and $rCBV_{max}$ (**E**) between different PD-L1 and Ki-67 status of PCNS-DLBCL

a high PD-L1 expression than those with a low expression in PCNS-DLBCL ($p<0.05$), whereas no significant differences were found in ADC_{mean}, $rADC_{min}$ and $rADC_{mean}$ values between low and high PD-L1 groups. The ADC_{mean} and $rADC_{mean}$ values in patients with a high Ki-67 LI were significantly lower than in those with a low Ki-67 LI (all $p<0.05$). As demonstrated in Table 3, ADC_{min} value for differentiating PD-L1expression status in PCNS-DLBCL with the cutoff value, sensitivity, specificity, and AUC of 0.55, 92.00%, 39.68%, and 0.642, respectively. The ADC_{mean} value to distinguish the patients with high Ki-67 LI from those with a low Ki-67 LI with the cutoff value, sensitivity, specificity, and AUC of 0.712, 73.97%, 60.00%, and 0.687, respectively. The diagnostic performance of $rADC_{mean}$ value in differentiation of low and high Ki-67 status in PCNS-DLBCL was similar

Table 3 Cutoff, sensitivity (%), specificity (%), and AUC of parameters for differentiation PD-L1 and Ki-67 status of PCNS-DLBCL

		ADC_{min}	ADC_{mean}	$rADC_{mean}$
PD-L1	Cutoff	0.55		
	Sen (%)	92.00		
	Spe (%)	39.68		
	AUC	0.642		
Ki-67	Cutoff		0.712	0.961
	Sen (%)		73.97	60.27
	Spe (%)		60.00	73.33
	AUC		0.687	0.671

Note: Sen, sensitivity; Spe, specificity; AUC, area under the curve

compared with ADC_{mean} (Cutoff value, sensitivity, specificity, and AUC of 0.961, 60.27%, 73.33%, and 0.671, respectively, $p>0.05$). The representative cases are illustrated in Figs. 2 and 3.

Discussion

In this study, we evaluated mMRI features, diffusion, and perfusion MR parameters of PCNS-DLBCL with different PD-L1 and Ki-67 expression statuses. We found that only diffusion MR can offer relevant information regarding PD-L1 and Ki-67 status in PCNS-DLBCL. However, their low diagnostic accuracy may limit their reliability in clinical practice.

PD-L1, a transmembrane protein, and its engagement with PD-1 plays a crucial role as an immune checkpoint in modulating the immune response against cancer [29]. Recent research has demonstrated that PD-L1 inhibitors offer a survival advantage over conventional standard therapy in patients with relapsed or refractory PCNSL [8, 30]. The expression of PD-L1 by tumor cells, with a cutoff value of 30% in PCNSL, has been identified as a promising biomarker for predicting the prognosis and therapeutic efficacy of immunotherapy, thereby aiding in patient selection [13]. Our result showed that the patients with high PD-L1 expression in PCNS-DLBCL tended to be younger than those with low PD-L1 expression, which was inconsistent with a previous report [13]. Additionally, no significant differences of all mMRI features were observed in low and high PD-L1status, indicating that the clinical application of mMRI in evaluating PD-L1 expression in PCNS-DLBCL is quite limited. Recent studies have shown that DWI-derived ADC value was weak inversed associated with PD-L1 status in HNSCC [23, 24]. However, as far as we are aware, there was no

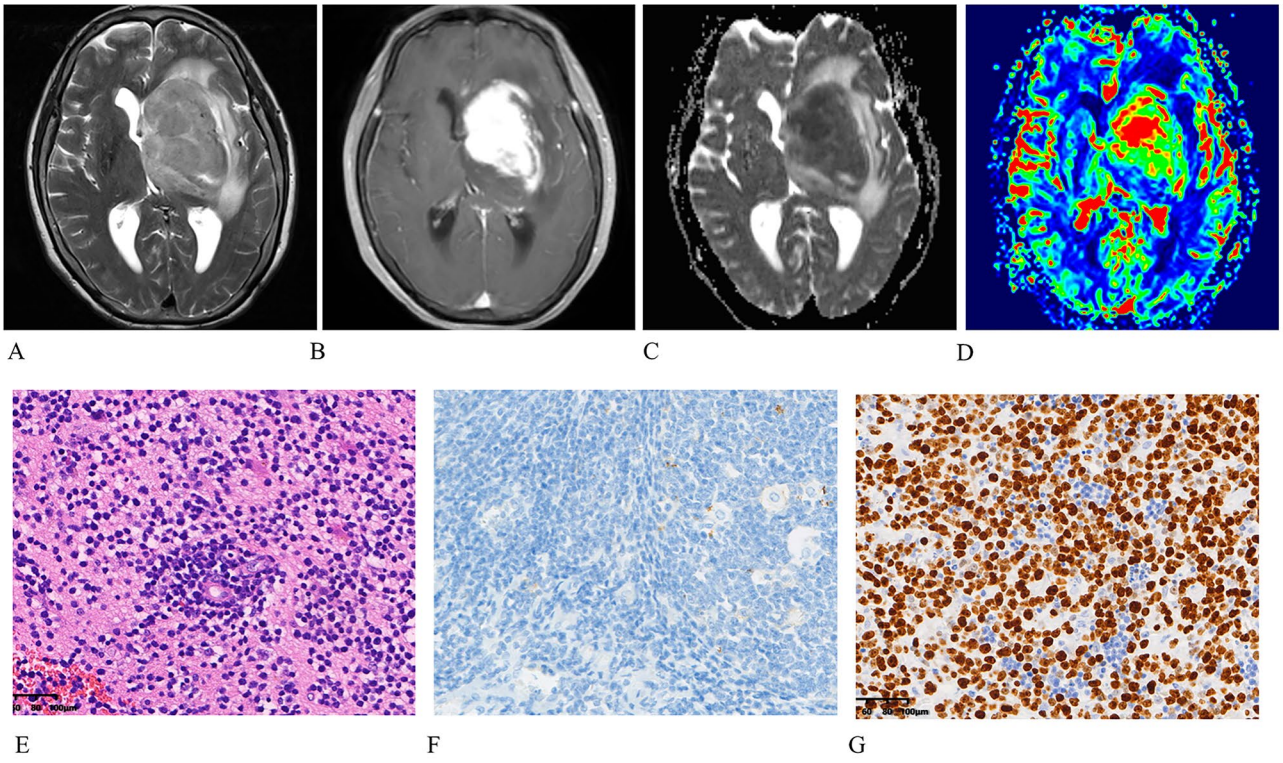

Fig. 2 T2WI (**A**) and contrast-enhanced T1WI (**B**) exhibit a prominently homogeneous contrast-enhancing tumor on the left basal ganglia region with mild-moderate edema. ADC map (**C**) demonstrates obviously decreased ADC values (ADC_{min}=0.435 × 10^−3mm^2/s, ADC_{mean}=0.435 × 10^−3mm^2/s, $rADC_{min}$=0.597, $rADC_{mean}$=0.680). CBV map (**D**) reveals a dramatically increased perfusion ($rCBV_{max}$ = 15.322). (**E**) Haematoxylin-eosin staining confirms the mass as a PCNS-DLBCL. (**F**) PD-L1 immunohistochemical test shows that approximately 3% of positive tumor cells for staining (**G**) Ki-67 immunohistochemical labeling demonstrates that around 80% of the cells exhibit positive nuclear staining. (magnification, × 20; scale bar, 100 μm)

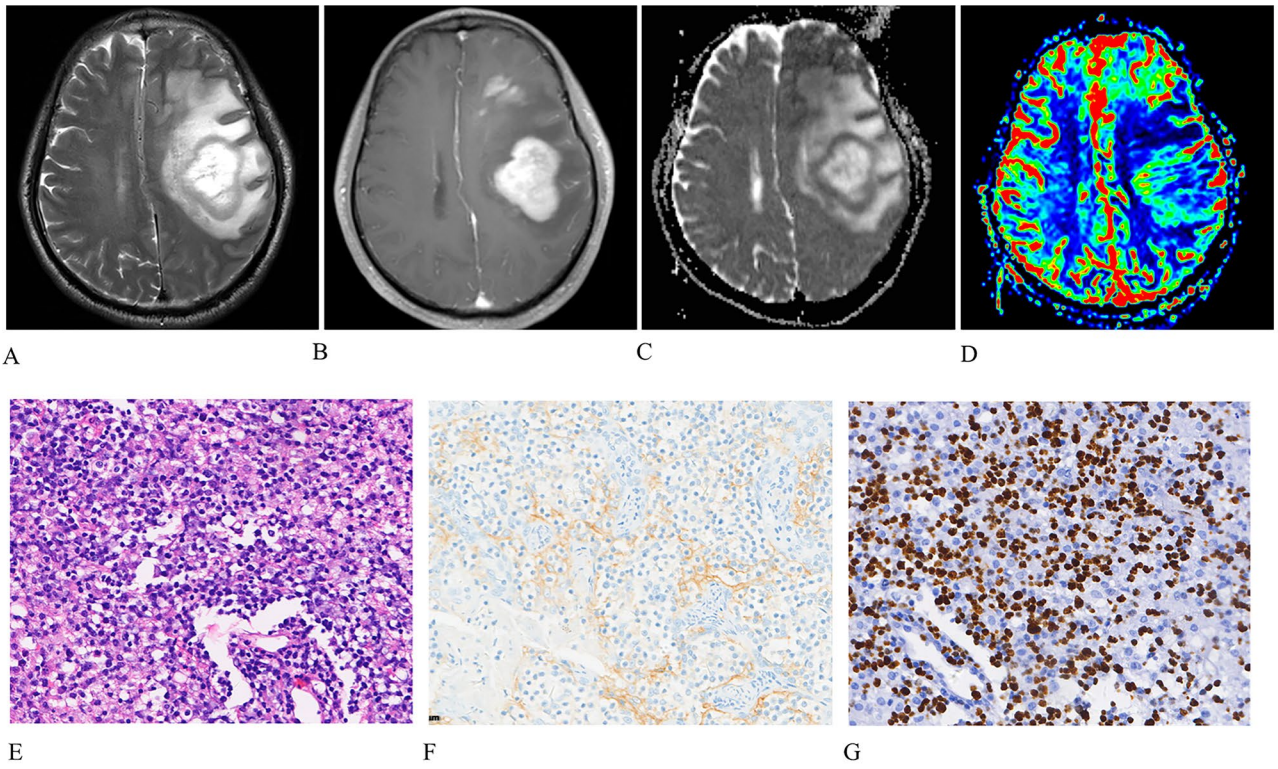

Fig. 3 T2WI (**A**) and contrast-enhanced T1WI (**B**) exhibit a tumor with marked and heterogeneous contrast-enhancement with severe oedema on the left frontal-parietal lobe. ADC map (**C**) demonstrates demonstrates mildly decreased ADC values (ADC_{min}=0.723×10^−3mm^2/s, ADC_{mean}=0.768×10^−3mm^2/s, $rADC_{min}$=1.006, $rADC_{mean}$=1.068). CBV map (**D**) reveals elevated perfusion ($rCBV_{max}$ = 8.582). (**E**) Haematoxylin-eosin staining identifies the mass as a PCNS-DLBCL. (**F**) PD-L1 immunohistochemical test demonstrates that approximately 60% of positive tumor cells for staining (**G**) Ki-67 immunohistochemical labeling reveals that around 60% of the cells exhibit positive nuclear staining. (magnification, × 20; scale bar, 100 μm)

study has demonstrated the correlation between ADC value and PD-L1 expression in PCNS-DLBCL. Our preliminary result showed that the ADC_{min} within PCNS-DLBCL was decreased in the low PD-L1 group, which was inconsistent with previous studies in HNSCC [23, 24]. Moreover, as proposed by Meng and Bortolotto et al. [31, 32]. , there was no significant difference in ADC values and different PD-L1 status in non-small cell Lung cancer. ADC values influenced by various factors, such as the intricate histopathological compartments, encompassing both cellular and extracellular aspects of tumors, tumor cell density, and so on, could be an explanation for these conflicting results in different solid tumors.

Ki-67, a nuclear antigen protein associated with cellular proliferation, has been extensively examined in diverse tumor types. Ki-67 LI with a threshold of 70% has demonstrated the ability to differentiate between DLBCL patients with favorable and unfavorable prognoses [15]. In this current study, we found that all mMRI features observed did not differ between low and high Ki-67 LI groups, which was in line with the prior studies [27]. DWI-derived ADC value has been recognized as a reliable biomarker inversely correlated with Ki-67 LI in some tumors [16, 19, 21, 26, 27, 33]. Our study showed that the ADC_{mean} and $rADC_{mean}$ were decreased in the high Ki-67 LI group compared with the low Ki-67 LI group in PCNS-DLBCL, which was in keeping with previous studies. However, these prior investigations involved only small case series and even include different histological types of lymphoma in their analysis [21, 22], which may result in potential bias to some extent. As we are aware, our present study was the first work that focused on the correlation of DWI and Ki-67 expression in PCNS-DLBCL.

According to the ROC curve analysis, the ADC values demonstrate a notably low predictive performance for PD-L1 and Ki-67 expression in PCNS-DLBCL. Furthermore, there is significant variability in the sensitivity and specificity of ADC_{min} value when distinguishing different PD-L1 statuses. Consequently, caution is warranted when interpreting the general applicability of our results. Regardless, DWI may be able to provide some degree of assistance in the detection of PD-L1 and Ki-67 status in PCNS-DLBCL, though the precise biological mechanisms remain uncertain and warrant further investigation in subsequent studies.

DSC-PWI can noninvasively provide the microvasculature characteristics information of tumors by rCBV value, and lesions characterized by elevated rCBV values

are generally of a higher grade and exhibit increased aggressiveness [34, 35]. Xing et al. reported that higher rCBV values were observed in the high Ki-67 LI group in patients with glioblastomas compared with the low Ki-67 LI group [27]. However, this significant correlation between rCBV values and Ki-67 LI was not observed in our research on PCNS-DLBCL. The differing results regarding the correlation between rCBV value and Ki-67 expression in glioblastomas and PCNSLs may be partially attributed to their distinct tumor vascularity characteristics. Glioblastomas are marked by tumor microvasculature and angiogenesis, while PCNSLs are characterized by a lack of tumor neovascularization due to its unique angiocentric growth pattern, where PCNSL cells cluster around pre-existing brain vessels [36]. To our knowledge, this was the first study that applied the DSC-PWI in the assessment of the correlation between perfusion-derived rCBV values and PD-L1 expression in brain tumors, and we found there was no difference between rCBV values and different PD-L1 statues in PCNS-DLBCL. As mentioned above, the unique biological growth pattern of PCNSL may explain our result to some extent. Nevertheless, these initial findings require confirmation through further multicenter studies, involving larger datasets of DSC-PWI investigations across various solid brain tumors.

Our study has several limitations that should be acknowledged. Firstly, the retrospective design of the study introduces inherent biases. Secondly, we utilized cut-off values of 30% and 70% for PD-L1 and Ki-67 LI overexpression, respectively. However, the optimal cut-off values for PD-L1 and Ki-67 in clinical setting remain uncertain, and the expression level of PD-L1 used IHC method across studies was inconsistent owing to the assays being dependent on the use of specific kinds of antibodies, staining conditions, cut-off values, companies, and companion instrument [14, 37]. Therefore, establishing a standardized and unified protocol for PD-L1 IHC testing in PCNSL is urgently needed. Thirdly, the DWI and DSC-PWI parameters measured from ROIs may not correlate well with histological fragments used for PD-L1 and Ki-67 immunohistochemistry on a site-specific basis. Therefore, MR-guided biopsy might be required to explore the associations between imaging parameters and molecular status accurately. Fourthly, the DWI with mono-exponential model we employed to assess the molecular statuses in this study may not adequately elucidate the complex microstructures of biological tissues. Therefore, further studies incorporating advanced MR techniques utilized by extended diffusion models, such as intravoxel incoherent motion and diffusion kurtosis imaging are recommended.

Conclusion

This present study demonstrated that diffusion parameters were significantly associated with PD-L1 and Ki-67 status in PCNS-DLBCL, however, the perfusion parameters and mMRI features were not correlated with these molecular statuses. PCNS-DLBCL with high PD-L1 expression tends to present a higher ADC_{min} value than those with low PD-L1 expression. Additionally, PCNS-DLBCL with high Ki-67 LI shows significantly reduced ADC_{mean} and $rADC_{mean}$ values in comparison to the group with low Ki-67 LI. Nonetheless, the effectiveness of ADC values in evaluating these molecular statuses in PCNS-DLBCL is relatively low, which somewhat limits their application in clinical practice.

Abbreviations

ADC	Apparent diffusion coefficient
ADC_{men}	Mean apparent diffusion coefficient
ADC_{min}	Minimum apparent diffusion coefficient
AUC	Area under the curve
CBV	Cerebral blood volume
DLBCL	Diffuse large B-cell lymphoma
DSC-PWI	Dynamic susceptibility contrast perfusion-weighted imaging
DWI	Diffusion-weighted imaging
HNSCC	Head and neck squamous cell carcinomas
ICC	Intraclass correlation coefficient
IHC	Immunohistochemical staining
mMRI	Morphological MRI
PCNS-DLBCL	Primary central nervous system diffuse large B-cell lymphoma
PCNSL	Primary central nervous system lymphoma
PD-1	Programmed cell death-1
PD-L1	Programmed cell death ligand-1
$rADC_{mean}$	Mean relative apparent diffusion coefficient
$rADC_{min}$	Minimum relative apparent diffusion coefficient
$rCBV_{max}$	Relative maximum cerebral blood volume
ROC	Receiver-operating characteristic

Acknowledgements

Not applicable.

Author contributions

ZX, DC and XZ conceived and designed the study. FW, LY, FY, and JK collected the data. XZ analyzed the data and wrote the paper. ZX and FW edit the paper. All authors read and approved the final manuscript for publication.

Funding

This work was supported by Scientific Research Project from the Education Department of Fujian Province (No. JAT210090), Natural Science Foundation of Fujian Province (No. 2021J01706), Joint Funds for the Innovation of Science and Technology, Fujian Province (No. 2021Y9093), Fujian Provincial Finance Project (No. 22SCZZX023).

Data availability

The dataset supporting the conclusions of this article is available upon request to the corresponding author.

Declarations

Ethics approval and consent to participate

The study was approved by the Medical Ethics Committee of the First Affiliated Hospital of Fujian Medical University. Individual consent was waived due to the retrospective study design. All procedures performed in this study involving human participants were in accordance with the Declaration of Helsinki.

Consent for publication
Not applicable.

Competing interests
The authors declare no competing interests.

Received: 29 February 2024 / Accepted: 22 August 2024
Published online: 26 August 2024

References

1. Deckert M, Engert A, Bruck W, Ferreri AJ, Finke J, Illerhaus G, Klapper W, Korfel A, Kuppers R, Maarouf M, et al. Modern concepts in the biology, diagnosis, differential diagnosis and treatment of primary central nervous system lymphoma. Leukemia. 2011;25(12):1797–807.
2. Olson JE, Janney CA, Rao RD, Cerhan JR, Kurtin PJ, Schiff D, Kaplan RS, O'Neill BP. The continuing increase in the incidence of primary central nervous system non-hodgkin lymphoma: a surveillance, epidemiology, and end results analysis. Cancer. 2002;95(7):1504–10.
3. Schlegel U, Schmidt-Wolf IG, Deckert M. Primary CNS lymphoma: clinical presentation, pathological classification, molecular pathogenesis and treatment. J Neurol Sci. 2000;181(1–2):1–12.
4. Gerstner ER, Batchelor TT. Primary Central Nervous System Lymphoma. In: *Primary central nervous system tumors: pathogenesis and therapy.* edn. Edited by Norden AD, Reardon DA, Wen PCY. Totowa, NJ: Humana Press; 2011: 333–353.
5. Schneider C, Pasqualucci L, Dalla-Favera R. Molecular pathogenesis of diffuse large B-cell lymphoma. Semin Diagn Pathol. 2011;28(2):167–77.
6. Juarez-Salcedo LM, Sandoval-Sus J, Sokol L, Chavez JC, Dalia S. The role of anti-PD-1 and anti-PD-L1 agents in the treatment of diffuse large B-cell lymphoma: the future is now. Crit Rev Oncol Hematol. 2017;113:52–62.
7. Maleki Vareki S, Garrigos C, Duran I. Biomarkers of response to PD-1/PD-L1 inhibition. Crit Rev Oncol Hematol. 2017;116:116–24.
8. Ansell S, Lesokhin A, Borrello I, Halwani A, Scott E, Gutierrez M, Schuster S, Millenson M, Cattry D, Freeman G, et al. PD-1 blockade with nivolumab in relapsed or refractory Hodgkin's lymphoma. N Engl J Med. 2015;372(4):311–9.
9. Westin J, Chu F, Zhang M, Fayad L, Kwak L, Fowler N, Romaguera J, Hagemeister F, Fanale M, Samaniego F, et al. Safety and activity of PD1 blockade by pidilizumab in combination with rituximab in patients with relapsed follicular lymphoma: a single group, open-label, phase 2 trial. Lancet Oncol. 2014;15(1):69–77.
10. Armand P, Nagler A, Weller E, Devine S, Avigan D, Chen Y, Kaminski M, Holland H, Winter J, Mason J, et al. Disabling immune tolerance by programmed death-1 blockade with pidilizumab after autologous hematopoietic stem-cell transplantation for diffuse large B-cell lymphoma: results of an international phase II trial. J Clin Oncology: Official J Am Soc Clin Oncol. 2013;31(33):4199–206.
11. Hawkes E, Grigg A, Chong G. Programmed cell death-1 inhibition in lymphoma. Lancet Oncol. 2015;16(5):e234–245.
12. Nayak L, Iwamoto F, LaCasce A, Mukundan S, Roemer M, Chapuy B, Armand P, Rodig S, Shipp M. PD-1 blockade with nivolumab in relapsed/refractory primary central nervous system and testicular lymphoma. Blood. 2017;129(23):3071–3.
13. Qiu L, Zheng H, Zhao X. The prognostic and clinicopathological significance of PD-L1 expression in patients with diffuse large B-cell lymphoma: a meta-analysis. BMC Cancer. 2019;19(1):273.
14. Kiyasu J, Miyoshi H, Hirata A, Arakawa F, Ichikawa A, Niino D, Sugita Y, Yufu Y, Choi I, Abe Y, et al. Expression of programmed cell death ligand 1 is associated with poor overall survival in patients with diffuse large B-cell lymphoma. Blood. 2015;126(19):2193–201.
15. Broyde A, Boycov O, Strenov Y, Okon E, Shpilberg O, Bairey O. Role and prognostic significance of the Ki-67 index in non-hodgkin's lymphoma. Am J Hematol. 2009;84(6):338–43.
16. Yang X, Zhu G, Yang Z, Zeng K, Liu F, Sun J. Expression of PD-L1/PD-L2 is associated with high proliferation index of Ki-67 but not with TP53 overexpression in chondrosarcoma. Int J Biol Mark. 2018;33(4):507–13.
17. Li J, Ge S, Sang S, Hu C, Deng S. Evaluation of PD-L1 expression level in patients with non-small cell lung cancer by F-FDG PET/CT radiomics and clinicopathological characteristics. Front Oncol. 2021;11:789014.
18. Lee J, Yoon Y, Seo S, Choi Y, Kim H. Soft tissue sarcoma: DWI and DCE-MRI parameters correlate with Ki-67 labeling index. Eur Radiol. 2020;30(2):914–24.
19. Xiao Z, Zhong Y, Tang Z, Qiang J, Qian W, Wang R, Wang J, Wu L, Tang W, Zhang Z. Standard diffusion-weighted, diffusion kurtosis and intravoxel incoherent motion MR imaging of sinonasal malignancies: correlations with Ki-67 proliferation status. Eur Radiol. 2018;28(7):2923–33.
20. Jiang J, Zhao J, Zhang Q, Qing J, Zhang S, Zhang Y, Wu X. Endometrial carcinoma: diffusion-weighted imaging diagnostic accuracy and correlation with Ki-67 expression. Clin Radiol. 2018;73(4):e413411–6.
21. Chong I, Ostrom Q, Khan B, Dandachi D, Garg N, Kotrotsou A, Colen R, Morón F. Whole tumor histogram analysis using DW MRI in primary central nervous system lymphoma correlates with tumor biomarkers and outcome. Cancers. 2019;11(10).
22. Schob S, Münch B, Dieckow J, Quäschling U, Hoffmann K, Richter C, Garnov N, Frydrychowicz C, Krause M, Meyer H, et al. Whole tumor histogram-profiling of diffusion-weighted magnetic resonance images reflects tumorbiological features of primary central nervous system lymphoma. Translational Oncol. 2018;11(2):504–10.
23. Meyer H, Höhn A, Surov A. Relationships between apparent diffusion coefficient (ADC) histogram analysis parameters and PD-L 1-expression in head and neck squamous cell carcinomas: a preliminary study. Radiol Oncol. 2021;55(2):150–7.
24. Rasmussen J, Olin A, Lelkaitis G, Hansen A, Andersen F, Johannesen H, Kjær A, Vogelius I, Specht L, Bentzen S, et al. Does multiparametric imaging with F-FDG-PET/MRI capture spatial variation in immunohistochemical cancer biomarkers in head and neck squamous cell carcinoma? Br J Cancer. 2020;123(1):46–53.
25. Ginat D, Mangla R, Yeaney G, Wang H. Correlation of diffusion and perfusion MRI with Ki-67 in high-grade meningiomas. AJR Am J Roentgenol. 2010;195(6):1391–5.
26. Yang X, Hu C, Xing Z, Lin Y, Su Y, Wang X, Cao D. Prediction of Ki-67 labeling index, ATRX mutation, and MGMT promoter methylation status in IDH-mutant astrocytoma by morphological MRI, SWI, DWI, and DSC-PWI. Eur Radiol. 2023;33(10):7003–14.
27. Xing Z, Huang W, Su Y, Yang X, Zhou X, Cao D. Non-invasive prediction of p53 and Ki-67 labelling indices and O-6-methylguanine-DNA methyltransferase promoter methylation status in adult patients with isocitrate dehydrogenase wild-type glioblastomas using diffusion-weighted imaging and dynamic susceptibility contrast-enhanced perfusion-weighted imaging combined with conventional MRI. Clin Radiol. 2022;77(8):e576–84.
28. Xing Z, Zhou X, Xiao Z, She D, Wang X, Cao D. Comparison of conventional, diffusion, and perfusion MRI between low-grade and anaplastic extraventricular ependymoma. AJR Am J Roentgenol. 2020;215(4):978–84.
29. Herbst RS, Soria JC, Kowanetz M, Fine GD, Hamid O, Gordon MS, Sosman JA, McDermott DF, Powderly JD, Gettinger SN, et al. Predictive correlates of response to the anti-PD-L1 antibody MPDL3280A in cancer patients. Nature. 2014;515(7528):563–7.
30. Lesokhin AM, Ansell SM, Armand P, Scott EC, Halwani A, Gutierrez M, Millenson MM, Cohen AD, Schuster SJ, Lebovic D, et al. Nivolumab in patients with relapsed or refractory hematologic malignancy: preliminary results of a phase ib study. J Clin Oncol. 2016;34(23):2698–704.
31. Bortolotto C, Stella G, Messana G, Lo Tito A, Podrecca C, Nicora G, Bellazzi R, Gerbasi A, Agustoni F, Grimm R et al. Correlation between PD-L1 expression of non-small cell lung cancer and data from IVIM-DWI acquired during magnetic resonance of the thorax: preliminary results. Cancers. 2022;14(22).
32. Meng N, Fu F, Sun J, Feng P, Luo Y, Wu Y, Li X, Yuan J, Yang Y, Liu H, et al. Sensitivity and specificity of amide proton transfer-weighted imaging for assessing programmed death-ligand 1 status in non-small cell lung cancer: a comparative study with intravoxel incoherent motion and F-FDG PET. Quant Imaging Med Surg. 2022;12(9):4474–87.
33. Yuan Y, Zeng D, Liu Y, Tao J, Zhang Y, Yang J, Lkhagvadorj T, Yin Z, Wang S. DWI and IVIM are predictors of Ki67 proliferation index: direct comparison of MRI images and pathological slices in a murine model of rhabdomyosarcoma. Eur Radiol. 2020;30(3):1334–41.
34. Boxerman J, Shiroishi M, Ellingson B, Pope W. Dynamic susceptibility contrast MR imaging in glioma: review of current clinical practice. Magn Reson Imaging Clin N Am. 2016;24(4):649–70.
35. Jain R, Gutierrez J, Narang J, Scarpace L, Schultz L, Lemke N, Patel S, Mikkelsen T, Rock J. In vivo correlation of tumor blood volume and permeability with histologic and molecular angiogenic markers in gliomas. AJNR Am J Neuroradiol. 2011;32(2):388–94.
36. K K K, J G S RVJ. Primary central nervous system lymphoma: radiologic-pathologic correlation. Radiographics. 1997;17(6).

37. Liu D, Wang S, Bindeman W. Clinical applications of PD-L1 bioassays for cancer immunotherapy. J Hematol Oncol. 2017;10(1):110.

Publisher's note